Optics Communications 369 (2016) 44–49

Contents lists available at ScienceDirect

Optics Communications

journal homepage: www.elsevier.com/locate/optcom

Rotation and conversion of transmission mode based on a rotatable elliptical core ring resonator

Bin Liu*, Yun-Feng Liu, Shu-Jing Li, Xing-Dao He

Jiangxi Engineering Laboratory for Optoelectronics Testing Technology, Nanchang Aeronautical University, China

A R T I C L E I N F O

Article history:
Received 7 October 2015
Received in revised form
26 January 2016
Accepted 16 February 2016
Available online 22 February 2016

Keywords:
Surface plasmon
Mode rotation
Optical resonators

A B S T R A C T

A compact plasmonic waveguide system consisting of a rotating elliptical core ring (ECR) coupled two metal-insulator-metal (MIM) waveguides is proposed. Influences of the eccentricity and rotation angle of the elliptical core on the transmission characteristics are studied in detail, by using Finite-Difference Time-Domain (FDTD) method. Compared with circular core in ring resonator, the elliptical core will lead to the asymmetric field distributions of intrinsic mode. Based on this, a 1 × 2 splitter is designed, in which the beam-splitting ratio can be adjusted by changing the eccentricity of the elliptical core. In addition, we find that the intrinsic mode of ECR rotate with elliptical core and gradually convert to its orthogonal mode. Separation of the pair orthogonal modes increases with growth of the eccentricity of the elliptical core. And, the higher order intrinsic mode corresponds to the shorter rotation angle of mode conversion.

1. Introduction

Surface plasmon polaritons (SPPs) are the electromagnetic surface waves that travel along the interface between metal and dielectric with an exponentially decay to the both sides. They are considered to have dramatically potential application in the realization of highly integrated optical circuits due to the prominent features that it can overcome the limit of traditional optical diffraction and manipulate optical wave on sub-wavelength scales [1]. Recently, various plasmonic devices have been focused and studied in experimentally or theoretically, such as Bragg reflectors [2,3], sensors [4], optical switching [5], filters [6], Y-shaped combiners [7], V-grooves [8,9], nanowires [10], etc.

Metal–Insulator–Metal (MIM) waveguides are important metallic nanostructures used to guide (SPPs) at the nanoscale [11–14]. The MIM waveguides are the hottest spot in recent years because of miniaturization and high level of integration of optical circuits. It could provide an interface between conventional optics and subwavelength electronic and optoelectronic devices. Waveguide-cavity coupling systems have been extensively studied on various platforms, including photonic crystal waveguides coupled microcavities systems [15], coupled whispering-gallery microresonators [16,17], self-coupled optical waveguide resonators [18,19], and so on. Recently, variety of waveguide-resonator coupled structures based on MIM plasmonic waveguides are proposed and their transmission characteristics analyzed [20–34], such as nanoring resonators, nanodisk resonators, square ring resonators, rectangular resonators, split ring core ring resonators, and so on. But, the influences of rotating resonant cavity on transmission characteristics have not been studied in detail.

In this paper, we study the transmission characteristics of a compact SPPs filter based on ECR resonators. The symmetry of ring resonator is broken with a rotatable elliptical core instead of circular core, which change the propagation path of SPPs in the resonator. The transmission properties of the system are simulated by FDTD method with grid size 2 × 2 nm. We analyze the influences of the eccentricity and rotation angle on transmission modes in detail. Then, a 1 × 2 beam-splitter with tunable splitting ratio is designed. In addition, with rotating the elliptical core, we observe rotation and conversion of transmission Modes in the structure.

2. The model

Fig. 1(a) shows that the structure is composed of two slits, an ECR resonator which is composed of an ellipse embedded in a nanodisk placed between the two MIM waveguides. d is width of waveguides, and w is distance between the boundary of the MIM waveguide and the ECR cavity, and R is radius of the cavity. L_1 and L_2 indicate the long axis and short axis of ellipse, respectively. We consider that variables are invariant along y direction. The index of white area is chosen as 1.52 (e.g. fused silica), and the medium of gray area accounts for silver. The dispersion equation of SPPs in the MIM structure can be described as [26]

---

* Corresponding author.
E-mail address: liubin_d@126.com (B. Liu).

http://dx.doi.org/10.1016/j.optcom.2016.02.033
0030-4018/

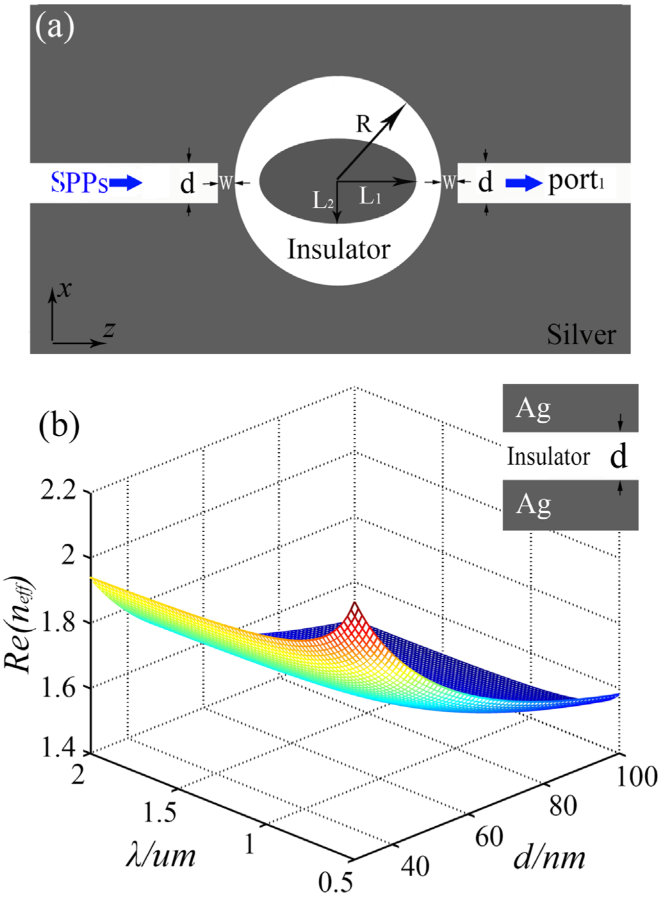

Fig. 1. (a) The schematic diagram of MIM waveguide coupled to an ECR, the gray and white areas are silver and insulator, respectively. (b) Dependence of Re(n_{eff}) of MIM structure on the wavelength of incident light and width d.

$$\frac{\varepsilon_0 P}{\varepsilon_m k} = \frac{1 - \exp(kd)}{1 + \exp(kd)},\ k = (\beta^2 - \varepsilon_0 k_0^2)^{1/2},\ p = (\beta^2 - \varepsilon_m k_0^2)^{1/2} \tag{1}$$

where β indicates the propagation constant of SPPs [35]. $k_0 = \frac{2\pi}{\lambda}$ is the wave number of light in the air, and λ is the wavelength of incident light. ε_0 and ε_m account for the dielectric constant of insulator and sliver, respectively. The frequency-dependent complex relative permittivity of silver is characterized by the Drude model [36]:

$$\varepsilon_m = \varepsilon_\infty - \frac{\omega_p^2}{\omega^2 + i\gamma\omega} \tag{2}$$

where $\varepsilon_\infty = 3.7$ stands for the dielectric constant at infinite angular frequency. $\omega_p = 9.1\text{eV}$ is the bulk plasma frequency which represents the natural frequency of the oscillations of free conduction electrons, and $\gamma = 0.018\text{eV}$ is the damping frequency of the oscillations. ω is the angular frequency of incident light. Effective refraction index (ERI) of the MIM structure is defined as $n_{eff} = \frac{\beta}{k_0}$, which can be calculated by Eq. (2). Fig. 1 shows the real part of n_{eff} as a function of d and λ. As seen from the figure, the n_{eff} decreases as the width d increases with the same wavelength λ.

3. Numerical simulation and analysis

The FDTD method is used to simulate the transmission characteristics. The grid size in the x and z directions are selected as 2×2 nm, which has enough precision in the following simulation. When the incident light transmits through input waveguide, part of the energy will be reflected and part of it coupled into ring cavity. Some modes which satisfy the resonant condition of ring cavity [37], can be coupled into $port_1$. The transmission-modes are called intrinsic modes of ring. In the paper, we use an elliptical core instead of circular core to break the symmetry of circular ring, which would impact the transmission of SPPs. Seen in Fig. 2(b), the ERI near short axis is lower than long axis due to the different widths of ring. Firstly, we study the influence of elliptical eccentricity on transmission characteristics of ECRs. We just perform 2D FDTD simulations by using Optiwave software with perfectly matched layer (PML) absorbing boundary conditions. The finite-difference time-domain (FDTD) method with fast Fourier transform is used to obtain the spectral response. The transmission spectrum of ECR with $L_1 = 140$ nm and $L_2 = 70$ nm is calculated in Fig. 2(a). There are two resonance modes in the wavelength range from 0.8 μm to 2 μm, which are called Mode 1 and Mode 2 corresponding to wavelengths 1626 nm and 935 nm, which contour profiles of magnetic field are depicted in Fig. 2(b) and (c). For Mode 2 in Fig. 2(c), we can observe the field distribution near long axis is stronger than short axis. The reason is the narrower waveguide width near long axis.

We add another MIM waveguide at the top of ECR as $port_2$, and the distance between the boundary of $port_2$ and ECR also is set as $w = 10$ nm, [shown in Fig. 3(a)]. Then, a 1×2 splitter is designed. The transmission spectrums of $port_1$ and $port_2$ are calculated in Fig. 3(b). We can see that there are two transmission peaks (Mode

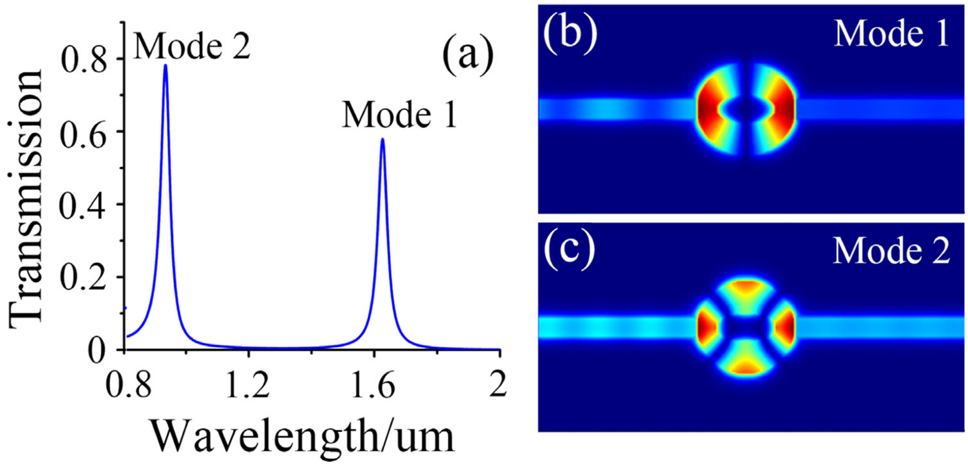

Fig. 2. (a) The transmission spectrum with $R = 220$ nm, $L_1 = 140$ nm, $L_2 = 70$ nm. (b, c) Fields $|H_y|^2$ at $\lambda = 1626$ nm (Mode 1) and $\lambda = 935$ nm (Mode 2).